Structures 91 (2026) 112679

Contents lists available at ScienceDirect

Structures

journal homepage: www.elsevier.com/locate/istruc

Energy-based seismic demand of multi-storey structures under pulse-like and non pulse-like ground motions

Raffaele Laguardia [a,*], Giulia Angelucci [b], Fabrizio Mollaioli [b]

[a] Department of Wellbeing, Health and Environmental Sustainability, Sapienza University of Rome, Via delle Fontanelle, Rieti, 02100, RM, Italy

[b] Department of Structural and Geotechnical Engineering, Sapienza University of Rome, Via Gramsci 53, Rome, 00197, RM, Italy

HIGHLIGHTS

- Seismic demand is quantified through the equivalent number of yielding excursions (n_{ye}).
- A large set of pulse-like and non-pulse like ground motions is used to evaluate n_{ye}.
- The influence of system type (SDOF vs MDOF) and hysteretic behavior is examined.
- Median n_{ye} is consistent across cases, but significant dispersion is observed.
- n_{ye} improves the estimation of elastoplastic ductility demand.

ARTICLE INFO

Keywords:
Energy-based
Equivalent cycles
Seismic demand
Pulse-like

ABSTRACT

Assessing seismic demand is a critical task in energy-based seismic design, as it depends on both ground motion characteristics and structural hysteretic properties. In recent years, growing attention has been devoted to demand evaluation through energy-related parameters, such as the equivalent number of yielding excursions (n_{ye}), particularly following the integration of energy-based approaches in the second-generation Eurocode drafts. Despite this interest, existing studies often rely on a limited number of structural typologies and ground motion records, with many focusing exclusively on SDOF systems. This work aims to bridge this gap by evaluating n_{ye} for MDOF structures through an extensive investigation of diverse structural configurations and a broad ground motion database. Specifically, this study investigates the cyclic seismic demand on multi-storey buildings subjected to 898 far-field records and 262 near-fault pulse-like records. The analyzed structures range from two to six storeys, with fundamental periods between 0.3 s and 1.5 s, and different hysteretic material models. The paper proposes two original formulations to estimate a global, system-level, n_{ye} parameter to be used within energy-based design frameworks alongside storey-level demands. The variability of this global parameter is extensively discussed by investigating its sensitivity to ground motion characteristics and by comparing MDOF results with their SDOF counterparts. The results show that median estimates remain quite stable and consistent with the literature, whereas the recorded dispersions are noteworthy. Furthermore, the practical utility of these descriptors is demonstrated: their integration enables a significantly more accurate estimation of strength reduction factors compared to the traditional Equal Displacement Approximation. Overall, the findings underscore the importance of n_{ye} for the development of energy-based methodologies and highlight the central role of uncertainty characterization in its estimation for future regulatory and code applications.

1. Introduction

Energy-Based Design (EBD) methodologies, pioneered by Housner [1] and formalized by Akiyama [2–4] into design procedures for both single- (SDOF) and multi-degree-of-freedom (MDOF) systems, provide a superior framework for the explicit quantification of cumulative structural damage. Unlike traditional approaches based on instantaneous maximum response parameters, such as peak force or deformation, EBD evaluates performance through integral metrics of the seismic demand imparted to a structure. This approach, extensively investigated in the subsequent decades [5–8], has been recently applied to innovative

* Corresponding author.
Email address: raffaele.laguardia@uniroma1.it (R. Laguardia).

https://doi.org/10.1016/j.istruc.2026.112679
Received 4 December 2025; Received in revised form 1 July 2026; Accepted 16 July 2026
Available online 23 July 2026

Abbreviations and Symbols

EBD	Energy Based Design
SDOF	Single-Degree of Freedom
MDOF	Multi-Degree of Freedom
GM	Ground Motion
FF	Far-Field
NF	Near-Field
PL	Pulse-Like
η	Cumulative plastic deformation ratio
$\overline{\eta}$	Average cumulative plastic deformation ratio among the storeys
μ	Ductility demand
μ_p	Plastic portion of ductility demand
$\overline{\mu}_p$	Average ductility among the storeys
E_H	Total plastic strain energy
n_{ye}	Equivalent number of yielding excursions
IMK	Ibarra-Medina-Krawinkler model
BL	Bilinear hysteretic model
PO	Peak-Oriented hysteretic model
POd	Peak-Oriented with degradation hysteretic model
AM	Arithmetic Mean
SE	SDOF-Equivalent
θ	Logarithmic median
β	Logarithmic dispersion
A_p	Maximum force in the elastoplastic system
A_e	Maximum force in the elastic system
EDA	Equal Displacement Approximation
CEE	Considering Energy Equivalence
RM	Median value of the ratio between A_p/A_e from TH and A_p/A_e from Eqs. (16) and (17).
RV	Dispersion of the ratio between A_p/A_e from TH and A_p/A_e from Eqs. (16) and (17).

seismic protection systems and structural capacity characterization [9, 10]. For a comprehensive overview of the EBD framework, the reader is referred to [11–13].

In particular, an energy-based perspective proves highly effective for the seismic assessment of structural systems located in the proximity of causative faults. In near-field (NF) regions, in fact, earthquake ground motions (GMs) frequently exhibit dominant pulse-like (PL), high-amplitude components, which are most prominent in fault-normal velocity waveforms. The damage potential of such ground motions diverges fundamentally from that of typical far-field (FF) records, where energy progressively accumulates over time. Indeed, velocity pulses, generated by the constructive interference of radiated waves due to fault rupture directivity, impart sudden, large energy demands that concentrate structural damage within a few large yielding excursions [14,15]. As a result, the total energy dissipated at the end of the ground motion primarily depends on the contribution of a few significant peaks within a narrow time window of the initial response phase [16–18]. While efforts have been devoted to characterizing PL ground motions [19,20], estimating their corresponding pulse periods [21–24], or investigating their effects on elastic and inelastic systems [25–28], the definition of a single, effective energy-based demand parameter remains a central challenge.

Originally developed for non-impulsive records, the cumulative plastic deformation ratio, η, was first introduced by Akiyama as a fundamental integral measure of the ductility levels sustained by a structure over the entire duration of an earthquake. Considering an ideal elasto-plastic SDOF system, η can be expressed as follows [3]:

$$\eta = \frac{E_H}{F_y u_y} \tag{1}$$

where E_H is the total plastic strain (hysteretic) energy absorbed by the system; F_y and u_y are the yielding force and displacement, respectively.

The η parameter is crucial for damage quantification; indeed, it is a comprehensive measure of the number and amplitude of the yielding excursions (and the resulting hysteretic cycles) undergone by the system during a seismic event. To ensure conceptual clarity, it is worth distinguishing between these terms: a 'yielding excursion' refers to each individual branch of the hysteretic curve that exceeds the yielding displacement, while a 'hysteretic cycle' typically represents a full reversal of loading. During a seismic event, hysteretic energy accumulates as a function of the number and varying amplitudes of these yielding excursions. To normalize these quantities, it is effective to define the 'equivalent number of yielding excursions (or cycles)' at a fixed displacement (or ductility) level that would produce the same cumulative hysteretic energy as the actual seismic action (e.g., a specific ground motion). In this work, we will refer to the equivalent number of yielding excursions, n_{ye}, defined as follows:

$$n_{ye} = \frac{\eta}{\mu_p} \tag{2}$$

where μ_p is the plastic portion of ductility demand μ (i.e., $\mu_p = \mu - 1 = (u_{max} - u_y)/u_y$) and u_{max} is the maximum displacement.

Several authors have dealt with this problem using similar or alternative approaches. McCabe and Hall [29] proposed the number of Equivalent Maximum Deformation Hysteretic (EMDH) cycles which is expressed as:

$$n_{ye}^{MH} = \frac{E_H}{F_y(u_{max} - u_y)} \tag{3}$$

It can be easily observed that Eqs. (3) and (2) are equivalent for an ideal SDOF elasto-plastic system. Kunnath and Chai [30] studied the influence of varying ductility levels and ground motion characteristics on the cyclic response of structures and proposed a new damage parameter that explicitly considers the shape of the hysteresis loop through a dimensionless parameter (α_h), leading to the following expression:

$$n_{cy}^{Ku} = \frac{E_H}{4\alpha_h \mu (F_y u_y)} \tag{4}$$

The main difference between Eqs. (4) and (2) lies in the presence of the α_h coefficient, whose values are discussed in [30], and the inclusion of the factor 4 in the denominator. Indeed, Eq. (4) quantifies the number of equivalent full cycles rather than the number of equivalent yielding excursions. A similar expression for the equivalent number of cycles incorporating the hysteretic loop shape was proposed by Dutta and Mander [31]. Their formulation, developed for the energy-based design of ductile reinforced concrete (RC) columns, explicitly considers the fatigue effects on structural damage due to different cycle amplitudes. An alternative assessment of equivalent cycles based on fatigue models was also proposed by Malhotra [32], who developed the following expression by adopting the Manson & Coffin [33] model:

$$n_{cy}^{Ma} = 0.5 \sum_k \left(\frac{u_k}{u_{max}}\right)^c \tag{5}$$

where u_k is the displacement at the k-th cycle and c is a parameter that accounts for fatigue effects.

A comprehensive review of existing methods for the quantification of n_{ye} can be found in [34]. However, the sensitivity of this parameter to specific seismic demand characteristics, especially considering impulsive GMs, requires further examination. Such events, indeed, typically induce high damage levels and localized plasticity that can affect the overall structural performance [35,36]. In light of this, Benavent Climent et al. [37] developed regression models for SDOF systems across a range of periods, utilizing near-field and far-field ground motion sets. Their best-fit analyses led to estimated values between 2.5 and 4.5 for NF cases, and approximately 3.5 to 6.0 for FF records, which is also in good agreement with the results from Akiyama [38]. Notably, it is observed that all the aforementioned methodologies for assessing the equivalent yielding excursions were originally developed and calibrated for SDOF systems. However, as far as the application of EBD methods for multi-storey framed structures is concerned, a systematic investigation into the behavior of MDOF systems is necessitated. Akiyama [3] initially dealt with this challenge by studying the number of yielding excursions on a five-story frame. The structure was modelled using a simplified stick-like model with each storey characterized by an ideal elasto-plastic behavior. Drawing from the results of a single seismic case study, he suggested a tentative design value of $n_{ye} = 2$. Utilizing the same approach, Akiyama [3] also investigated the influence of strain hardening and cyclic deterioration properties on the assessment of η, showing that its value reduces as the hardening ratio increases or when the system exhibits degrading hysteretic behavior. In subsequent studies, Akiyama [38,39] expanded upon his previous findings by performing a parametric analysis of multi-story shear-type frames modelled as “flexible-stiff mixed multi-storey systems” by connecting perfectly elastic and elastic-perfectly plastic springs in parallel at each storey. Through this parametric investigation, Akiyama concluded that the presence of a relevant elastic component increases the n_{ye} value while for purely elasto-plastic systems n_{ye} is at most equal to 4. Despite the availability of predictive equations for the equivalent number of yielding excursions [12,40,41], the current literature provides only limited guidance for the comprehensive characterization of n_{ye} in MDOF systems. A significant advancement in this field is the recent work by Benavent-Climent et al. [42], who derived analytical formulations for storey-level equivalent number of yielding excursions by extending previously established SDOF-based predictive laws. Nonetheless, the generalization of these models is currently hindered by the limited structural typologies investigated and the narrow variability of the seismic datasets employed. A deeper investigation of n_{ye} is, therefore, highly desirable, considering its key role within EBD frameworks for both the assessment of existing structures and the design of new ones. On this point, Donaire-Ávila et al. [43] emphasized that a robust EBD framework must explicitly incorporate the inherent uncertainties of all demand parameters, a prerequisite for developing probabilistic methodologies that can be effectively integrated into international design codes and performance-based approaches. This urgency is now even more pressing due to the recent integration of energy-based methodologies into the second generation of Eurocodes for the design of supplemental damping systems [37,44]. Specifically, the seismic demand at the i-th storey of a building will be quantifiable by means of the following expression:

$$u_{max,i,1} = u_{y,i} + \left(\frac{E_{H,i}}{4F_{y,i}}\right) \quad (6)$$

where $u_{max,i}$, $u_{y,i}$, $E_{H,i}$ and $F_{y,i}$ are the maximum first-mode inter-storey displacement, the yielding inter-storey displacement, the hysteretic energy demand, and the lateral force capacity at the i-th storey of the frame equipped with dissipative device, respectively. By normalizing this equation by $u_{y,i}$ and adopting Eqs. (1) and (2) to define storey-level cumulative plastic deformation ratio and yielding excursions (i.e., η_i and $n_{ye,i}$), it can be demonstrated that the formulation is predicated upon the implicit assumption of $n_{ye,i} = 4$:

$$\frac{u_{max,i,1}}{u_{y,i}} = 1 + \left(\frac{E_{H,i}}{4F_{y,i}u_{y,i}}\right) \quad (7)$$

$$\mu_i = 1 + \mu_{p,i} = 1 + \frac{\eta_i}{n_{ye,i}} \quad (8)$$

where $\mu_{p,i}$ is the plastic ductility at i-th storey.

Motivated by the aforementioned limitations in the current literature and the recent adoption of EBD in seismic codes, this paper aims to shed some light on the energy-based parameter n_{ye} by addressing the following specific research objectives:

- To investigate the variability of n_{ye} across both SDOF and MDOF structures. For MDOF systems, local values (at each storey) and global values (derived from two alternative formulations) are evaluated.
- To assess the influence of structural characteristics on the estimation of n_{ye}, specifically focusing on the number of storeys (2, 4, and 6) and representative material behaviors (elasto-plastic, peak-oriented, and peak-oriented with degradation).
- To explore the impact of impulsive and non-impulsive ground motions on the estimation of $n_{ye,i}$, using an extensive database of 898 FF and 262 NF PL records.
- To evaluate the effectiveness of adopting MDOF-derived n_{ye} values to improve the estimation of strength reduction factors for design applications.

The paper is organized as follows: Section 2 details the case-study structures and their numerical modeling assumptions; Section 3 describes the GM database adopted; Section 4 discusses available formulations and introduces new expressions for the n_{ye} assessment in SDOF and MDOF structures; Section 5 presents and discusses the numerical results obtained; finally, conclusions are drawn in Section 6.

2. Numerical modeling of case study structures

In order to investigate the variability of n_{ye} upon structural characteristics, several multi-storey structures with different dynamic and hysteretic properties are analysed in this work. Two-, four- and six-storey framed structures, characterized by different fundamental periods T (specifically 0.3 s, 0.5 s, 1 s and 1.5 s), are considered along with their corresponding SDOF systems equivalent to the first mode. The selected structural typologies reflect the statistical prevalence of the Italian RC residential building stock, which is predominantly characterized by low-to-mid-rise configurations up to five storeys [45]. Moreover, the adopted period range is representative of both bare and infilled RC frames as non-structural masonry infills significantly enhance global lateral stiffness and shift fundamental periods toward shorter values.

The structural response of the analyzed structures was simulated in OpenSees [46] employing multi-storey stick-like models. It is noted that, while this stick-like shear-type idealization is computationally efficient for large-scale parametric assessments of energy demand, it entails simplifications regarding the finite flexural stiffness of the beams and the axial deformation of the columns. Nevertheless, it provides a satisfactory approximation of the global seismic response (e.g., inter-storey drift profiles and global energy dissipation) for the regular, low-rise frames investigated herein [47]. To evaluate the sensitivity of n_{ye} to diverse dissipation mechanisms, each storey was assigned a hysteretic Ibarra-Medina-Krawinkler (IMK) constitutive model [28]. Specifically, a Bilinear (BL) variant and a Peak Oriented model, either without (PO) or with stiffness and strength degradation (POd), were adopted. The aim was to encompass hysteretic properties representative of different structural typologies and materials, such as steel and RC.

Fig. 1 illustrates the adopted IMK models along with the key parameters required for their definition, for which established predictive equations, derived from extensive experimental datasets, are available [48,49]. Moreover, Fig. 1 illustrates the parameters needed to assess n_{ye} through Eqs. (1)–(2) for the adopted models (bilinear and peak-oriented), where E_H represents the cumulative area enclosed by the force-displacement hysteresis loops. Considering the goals of this work and the need to simulate a large number of structures, only the yielding force and displacement at each storey were designated as the varying

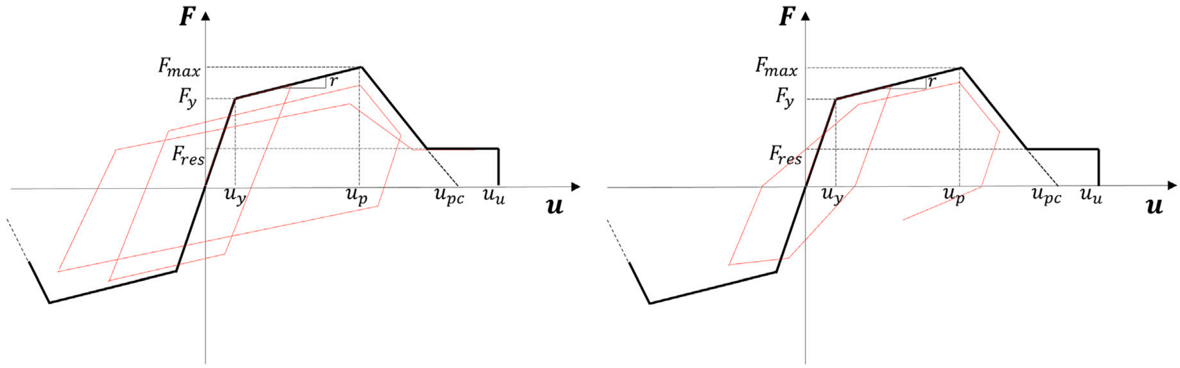

Fig. 1. Adopted IMK model: (A) Bilinear IMK; (B) Peak-oriented IMK.

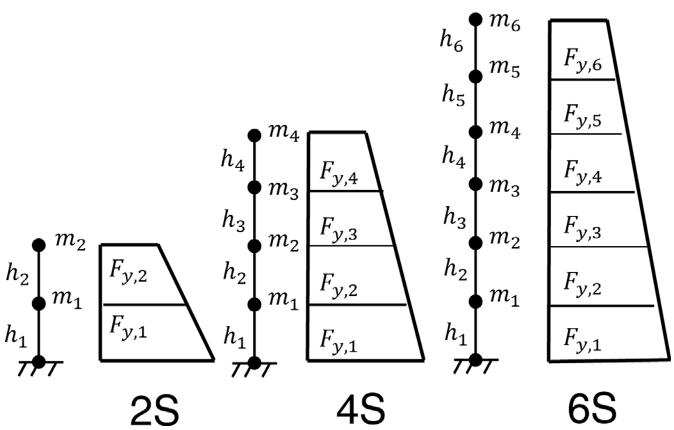

Fig. 2. Adopted force distribution for two-storey (2S), four-storey (4S) and six-storey (6S) structures.

parameters. All other monotonic and hysteretic parameters were constrained to reasonable, fixed values based on engineering judgement. A linear distribution of the yielding force with a 2:1 ratio between the base and the top storeys was assumed along the building's height, as shown in Fig. 2.

The specific value at each storey was assessed according to the following criteria:

$$u_{y,i} = \theta_{y,i} h_i \quad (9a)$$

$$F_{y,1} = \alpha M \quad (9b)$$

$$F_{y,i}^{Lin} = F_{y,1}\left(1 - 0.5\frac{i-1}{N-1}\right) \quad if \quad i > 1 \quad (9c)$$

where $\theta_{y,i}$, m_i, h_i are the yielding chord rotation, mass and height of the i-th storey, M is the total mass of the structure and α is a parameter governing the base yielding force value. It is noted that Eq. 9a is derived under the assumption of shear-type behavior for the MDOF system. The linear lateral strength profile was adopted as a primary approach, which is consistent with the fundamental-mode dominance typical of the investigated low-rise structures with regular stiffness distributions. However, it is recognized that the assumed capacity distribution might significantly affect the concentration of plastic demands along the building height. In this regard, it is worth mentioning that current EBD methodologies, including the forthcoming second-generation Eurocodes, often advocate for an 'optimal' strength distribution [38,39,50] aimed at enforcing a uniform energy dissipation ratio across the storeys. Investigating how alternative distributions affect the global and local evaluation of n_{ye} is an objective of ongoing research. Table 1 summarizes the structural

Table 1
Description of the modelling parameters adopted for each structural typology: first mode period T, base shear coefficient α, yielding chord rotation θ_y.

	SDOF		2S		4S		6S	
T[s]	α	θ_y	α	θ_y	α	θ_y	α	θ_y
0.3	0.75	0.5%	1.2	0.5%				
0.5	0.28	0.5%	0.44	0.5%	0.77	0.5%		
1	0.07	0.5%			0.18	0.5%	0.27	0.5%
1.5	0.03	0.5%					0.12	0.5%

properties adopted for the two-, four-, and six-storey frames with different elastic periods, alongside the parameters of the corresponding SDOF model adopted for comparison. The parameters listed in Table 1 were obtained by fixing the yield rotation at 0.5% and subsequently calibrating the α coefficients to match the target elastic periods. This 0.5% value was selected as a representative compromise to account for the typical response of both steel and reinforced concrete structures, including existing ones, within a single, simplified parameterization. As far as the other parameters of the IMK models are concerned, the following values were assumed: $\theta_p = 4\%$, $\theta_{pc} = 10\%$, $r = (F_{max} - F_y)/\theta_p = 5\%$ and degrade parameter d = 1 for the POd cases and d = 0 for the others.

3. GMs database

An extensive GM database compiled from internationally recognized repositories is employed to ensure a broad representation of global seismic events, specifically the Engineering Strong-Motion (ESM) database, the Italian Accelerometric Archive (ITACA), the Pacific Earthquake Engineering Research Center (PEER) Ground Motion Database and the Center for Engineering Strong Motion Data (CESMD). The selection comprises 898 FF and 262 NF records with pulse-like components. The methodology adopted here follows the established framework for cloud analysis using unscaled ground motions. This approach is primarily motivated by the need to mitigate statistical bias and spectral distortion often introduced by excessive amplitude scaling within spectral matching procedures [51]. Employing as-recorded ground motions, indeed, ensures the inherent record-to-record variability for robust probabilistic seismic demand estimation while preserving physically consistent seismotectonic features. To maintain comparability, seismological constraints were applied to both datasets. Specifically, the moment magnitude (M_w) was constrained between 5.0 and 8.0 to focus on the range that generally dictates the hazard in regions of medium-to-high seismicity. The site conditions included soil preferred shear-velocities (V_{S30}) between 160 m/s and 1000 m/s, with the largest portion of the records belonging to Eurocode 8 soil classes B and C. Fig. 3 illustrates the distributions of the key intensity measures (IMs), encompassing both

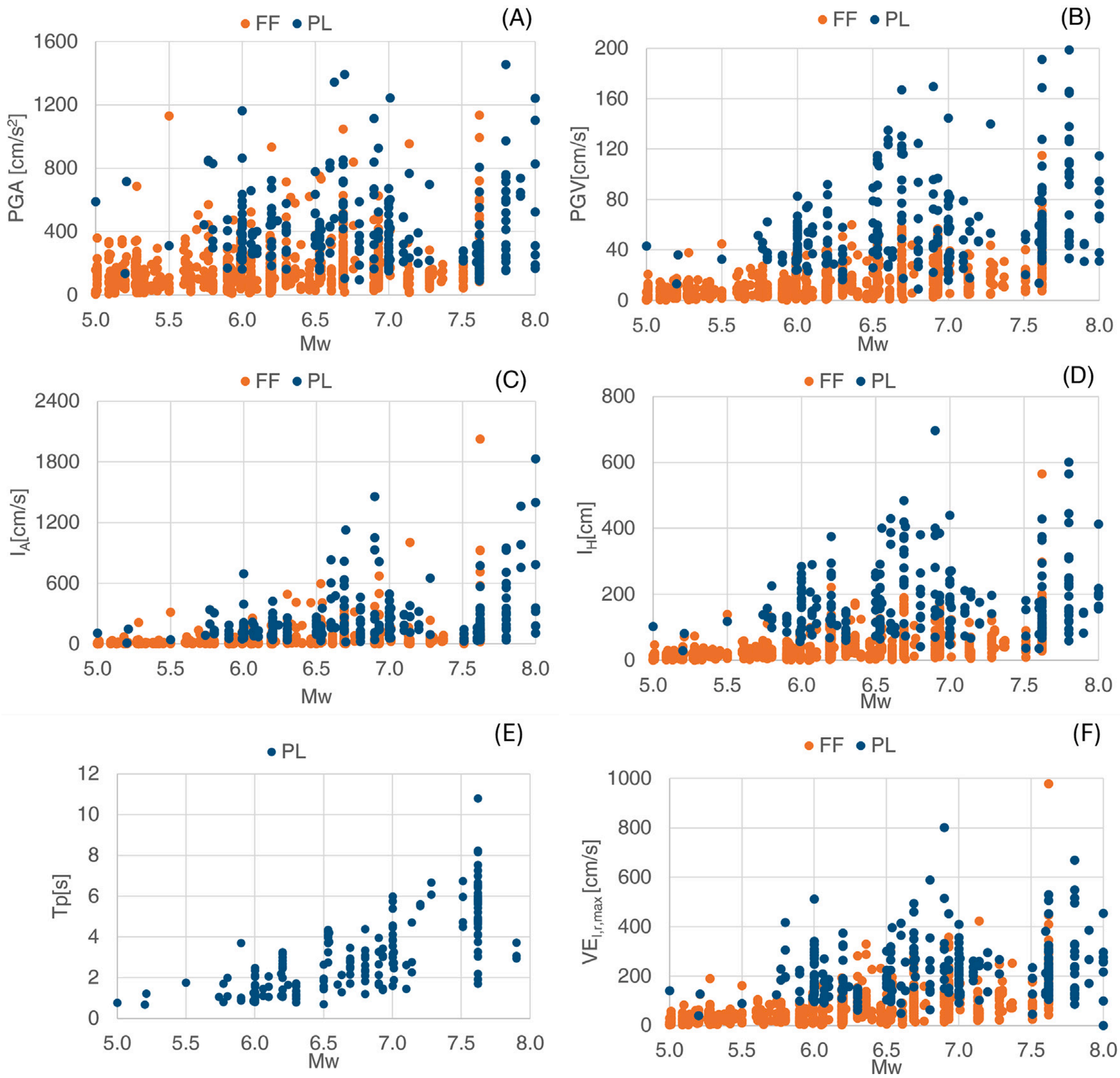

Fig. 3. Intensity measures of adopted GM datasets: (A) peak ground acceleration (PGA); (B) peak ground velocity (PGV); (C) Arias intensity (I_A); (D) Housner intensity (I_H); (E) pulse period (T_p); peak relative input energy equivalent velocity ($VE_{Ir,\max}$).

peak-based scalar and integral metrics to characterize the seismic input. In particular, velocity-based IMs (i.e., Peak Ground Velocity (PGV) and Housner Intensity (I_H)) have demonstrated superior efficacy in representing the structural demand imposed by impulsive near-fault signals since pulse-like components are typically detected in the velocity time history [28,47]. For the sake of comparison with other velocity-based IMs, the peak relative input energy ($E_{Ir,\max}$) is expressed in terms of its equivalent velocity ($VE_{Ir,\max}$), serving as a proxy for the maximum seismic energy demand that can be transmitted to the structure. For alternative energy-based intensity measures, the interested reader is referred to [28,52]. It is observed that mean intensity levels are generally higher for the PL dataset due to concentrated energy demand within a narrow time interval and large PGV compared to FF records of the same magnitude. Nevertheless, this disparity is not deemed to compromise the validity of the results, as the study aims to quantify the equivalent number of yielding excursions over instantaneous peak demands.

As far as the NF dataset is concerned, the closest site-to-source distance (D_f) is less than 30 km. The fault-normal horizontal seismic signal components were processed using the Variational Mode Decomposition (VMD) technique [24]. This signal processing method effectively decomposes near-fault seismic ground velocity records to identify embedded impulsive modes and estimate the associated pulse period (T_p) [53]. It is also highlighted that T_p extracted via the VMD technique closely aligns with established benchmark methods, such as the wavelet-based approach by Baker [22]. The relationship between the identified pulse periods and moment magnitude is illustrated in Fig. 3. In agreement with previous findings (e.g., [21,22,24]), impulsive near-fault earthquakes exhibit significantly high T_p values. Also a clear correlation exists between magnitude and the period associated with the peak energy spectral ordinate (E_{Ir}) as the peak value of the relative input energy spectrum is commonly attained in the vicinity of T_p, which, in turn, scales proportionally with earthquake magnitude [54].

Notably, while only 20% of PL records exhibit T_p values within the initial elastic period range of the analyzed structures, inelastic period elongation significantly shifts the effective dynamic response toward longer periods. By considering a period extension up to 4T (6.0 s), consistent with the integration limits proposed for the Average Spectral Acceleration ($AvgS_a$) in the study of infilled frames [55], this interval encompasses the pulse period for 91% of the PL dataset.

4. Cyclic demand assessment for SDOF and MDOF structures

This study aims to quantify the number of yielding excursions for different structural systems subjected to far-field and near-field pulse-like ground motions by adopting a broad database. The primary focus is on MDOF systems, but a comparative analysis is also provided against SDOF systems with equivalent dynamic properties to improve understanding. The n_{ye} formulations adopted for MDOF and SDOF systems are presented in the following sections.

4.1. SDOF structures

Despite the availability of various alternative formulations for the evaluation of n_{ye} in SDOF systems, the formulation provided in Eq. (2) was adopted for the purposes of this study, due to its simplicity and its extensive use in the existing literature. This choice is further substantiated by the availability of predictive equations, such as those proposed by Manfredi [40] and Manfredi et al. [41], which express n_{ye} as a function of a seismological parameter:

$$n_{ye}^{MF} = 1 + c_1 I_d \sqrt{\frac{T_{NH}}{T_s}} (R-1)^{c_2} \tag{10}$$

where T_{NH} is the initial period of the medium period region pertaining to the Newmark and Hall spectral representation, T_s is the period of the SDOF system, R is the force reduction factor, I_d is a seismological parameter defined in [41] whereas c_1 and c_2 are parameters calibrated for near-field and far-field GMs (i.e., $c_1 = 0.23$ and $c_2 = 0.4$ for near-field; $c_1 = 0.18$ and $c_2 = 0.6$ for far-field according to [40,41]).

4.2. MDOF structures

For MDOF systems, contributions specifically aimed at assessing n_{ye} are relatively few, primarily limited to the foundational work of Akiyama [3,38,39]. Specifically, based on the modeling approach for flexible-stiff mixed multi-storey systems [38,39], he proposed the following predictive equation for n_{ye}:

$$\frac{\eta}{\mu_p} = 4 + r_q \qquad r_q \leq 1 \tag{11a}$$

$$\frac{\eta}{\mu_p} = 8 \sim 12 \qquad r_q > 1 \tag{11b}$$

where $r_q = \frac{fQ_m}{sQ_y}$ is the ratio of the maximum force in the elastic part, fQ_m, and the yield strength of the elasto-plastic part, sQ_y. Utilizing Eq. (11), Benavent-Climent et al. [42] have recently proposed a predictive equation that formally extends Eq. (10) to MDOF systems.

In this latter case, rigorous investigation into the values assumed by the n_{ye} parameter is essential at two distinct scales: quantifying the local demand at the storey level and attempting the evaluation of a global n_{ye} value for the entire structure.

The yielding excursion at the i-th storey can be defined as follows:

$$n_{ye,i} = \frac{\eta_i}{\mu_{p,i}} = \frac{E_{H,i}}{F_{y,i} u_{y,i} \mu_{p,i}} \tag{12}$$

In this study, the global evaluation of the n_{ye} parameter was carried out by adopting two alternative approaches: one based on the arithmetic mean of the storey-level n_{ye} values (i.e., n_{ye}^{AM}), and the other based on an equivalence with a corresponding SDOF system (i.e., n_{ye}^{SE}). Regarding this latter, the inherent structural regularity and low- to medium-rise configuration (up to 6 storeys) of the analyzed frames justify the adoption of a simplified SDOF reduction as a representative global indicator. The two formulations are, respectively, expressed as follows:

$$n_{ye}^{AM} = \sum_i n_{ye,i}/N \tag{13}$$

$$n_{ye}^{SE} = \frac{E_H}{F_{ye} u_{ye} \overline{\mu}_p} \quad ; \quad F_{ye} = F_{y,1} \quad ; \quad u_{ye} = F_{y,1} \frac{\mathrm{T}^2}{4M\pi^2} \tag{14}$$

where N is the number of storeys, $\overline{\mu}_p$ is the average plastic ductility among the storeys and M is the mass of the structure.

In the remainder of this paper, Eq. (13) will be referred to as the AM (Arithmetic Mean) method and Eq. (14) as the SE (SDOF Equivalence) method.

5. Numerical results

This section presents the results of the Nonlinear Time-History Analyses (NLTHAs) performed on the structural models defined in Section 2 and subjected to the ground motions described in Section 3. The resulting n_{ye} values, obtained via the methodologies outlined in Section 4, are displayed and discussed for both SDOF and MDOF systems. It is noted that, to ensure the numerical stability and physical consistency of the results, a filtering procedure was applied to exclude records leading to extreme responses ($\eta_{ye} \geq 20$ or $\overline{\mu}_p \geq 10$). These cases, which typically represent less than 10% of the total analyses (reaching a peak of 15% on 6 storey structures at T = 1s for PL motions with PO and POd models), were discarded to avoid potential bias from localized numerical convergence issues in the extensive parametric study.

5.1. Number of yielding excursions

This section discusses the values of the equivalent number of yielding excursions across the investigated structural models using the alternative formulations introduced in Section 4. Descriptive statistics of the data samples obtained from the analyses are used for this purpose along with a technique widely used in the literature [3,11]. This latter approach involves assessing n_{ye} over a broad set of data points by plotting the results on an η/μ_p (cumulative plastic deformation ratio versus plastic ductility) plane and performing a linear regression on the resulting distribution. For SDOF systems, Eq. (2) clearly establishes that the slope of the linear regression yields an estimate of n_{ye}. This methodology is directly extendable to MDOF systems, provided that the average values across all storeys are considered for μ_p (i.e., $\overline{\mu}_p$) and η (i.e., $\overline{\eta}$).

5.1.1. Assessment through η/μ_p slopes

A representative application of this approach is shown in Fig. 4, where the η/μ_p values and the resulting linear regression derived from the FF and PL GMs are presented. The lower row shows the results for the two-storey (2S), four-storey (4S) and six-storey (6S) MDOF systems with the BL hysteretic model and using the AM approach; the upper row presents the results for the corresponding SDOF systems (1S). It is immediately evident that this representation not only provides a rough estimation of n_{ye} across a wide range of data points but also facilitates the identification of dominant trends, e.g., in Fig. 4 the consistently lower n_{ye} values obtained from the PL GM set (blue line) compared to those resulting from the FF GM set (red line). This trend can be attributed to the inherent nature of impulsive seismic demand, often characterized by a short effective duration and large displacement excursions [17,22]. In PL events, the seismic energy is delivered in a few high-intensity pulses that push the structure toward high peak ductility levels with minimal cyclic repetition and limited hysteretic energy. In contrast, FF motions typically trigger a multi-cycle response that accumulates significant hysteretic energy through numerous moderate excursions, resulting in higher n_{ye} values.

Fig. 5, along with Tables 2–4, presents the n_{ye} values derived from the η/μ_p slope of the linear regression applied to all investigated models

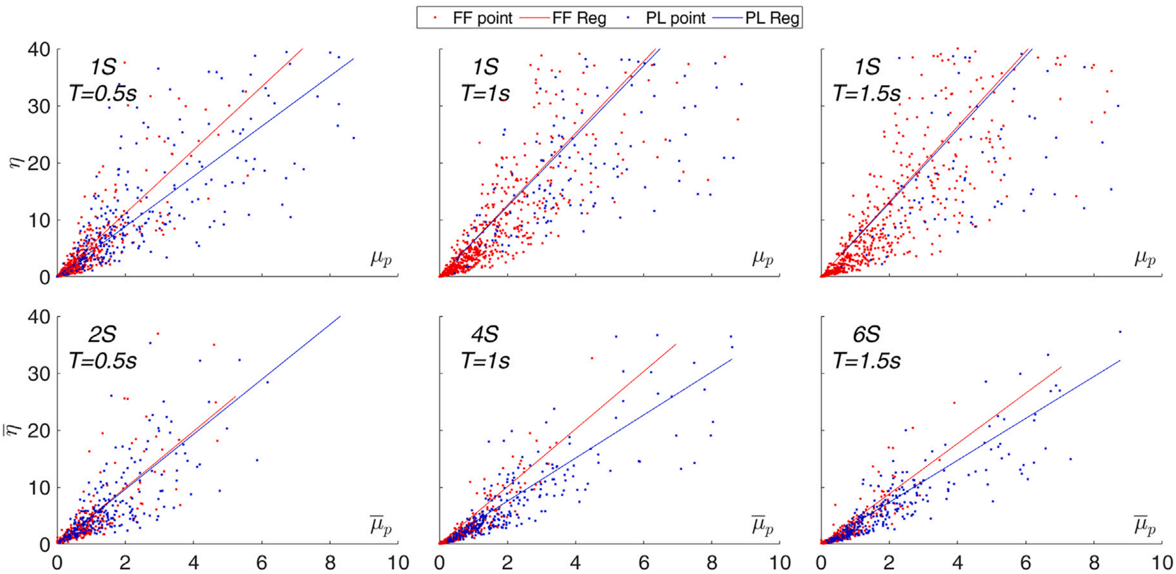

Fig. 4. η/μ_p values and linear regression for FF and PL GMs assessed through Eq. (2) for SDOF systems and through Eq. (13) for MDOF systems: case studies with Bilinear hysteretic behavior.

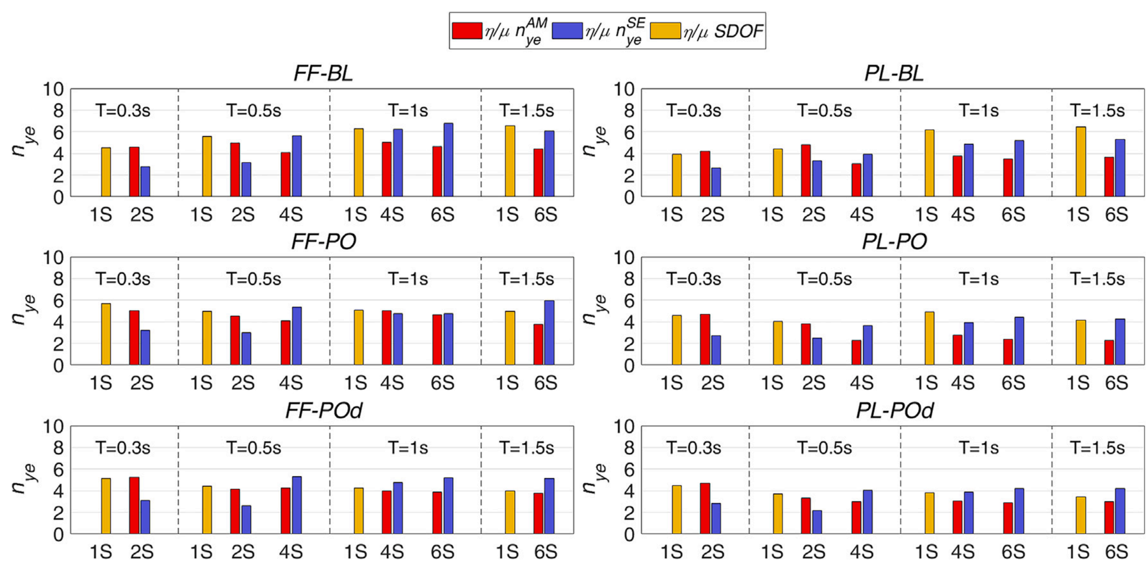

Fig. 5. η/μ_p values for FF and PL GMs considering all the models.

and structures, following the previously described technique. For SDOF systems, the calculated n_{ye} values typically fall within a range of 4 to 7. On the other hand, MDOF systems exhibit greater variability, with n_{ye} spanning approximately 2 to 7. Nonetheless, while the resulting values are notably influenced by the specific global assessment approach employed (AM or SE), the differences among the BL, PO, and POd models were found to be comparatively small.

With the aim of identifying the most suitable methodology for quantifying n_{ye} in MDOF structures, a critical issue where limited guidance is offered by existing literature, further investigation was pursued. Fig. 6 compares the η/μ_p values (derived from Fig. 5) by contrasting the results from SDOF models (i.e., n_{ye}^{SDOF}) with those from MDOF models (i.e., n_{ye}^{MDOF}) having identical fundamental periods. The median, mean, and coefficient of variation (C.o.V.) of the ratio between SDOF and MDOF values are summarized in Table 5, providing the necessary metrics for evaluating the consistency of the global MDOF assessment approaches. The results indicate that the AM method yields slightly lower values compared to SDOF models (with a median ratio between 0.77 and 0.91);

Table 2
$\frac{\eta}{\mu_p}$ numerical values for FF and PL GMs for SDOF structures.

$\frac{\eta}{\mu_p}$	SDOF - FF			SDOF - PL		
T[s]	BL	PO	POd	BL	PO	POd
0.3	4.55	5.70	5.15	3.9	4.61	4.45
0.5	5.56	4.97	4.44	4.40	3.70	3.70
1	6.29	5.06	4.27	6.17	4.94	3.83
1.5	6.58	4.99	3.98	6.45	4.15	3.43

Table 3
$\frac{\eta}{\mu_p}$ numerical values for FF and PL GMs using AM approach for MDOF structures.

$\frac{\eta}{\mu_p}$	2S-FF			4S-FF			6S-FF			2S-PL			4S-PL			6S-PL		
T[s]	BL	PO	POd	BL	PO	POd	BL	PO	POd	BL	PO	POd	BL	PO	POd	BL	PO	POd
0.3	4.59	5.05	5.23							4.19	4.70	4.29						
0.5	4.95	4.52	4.15	4.07	5.19	4.26				4.81	4.05	3.32	3.05	2.29	2.99			
1				5.05	4.15	3.96	4.65	4.27	3.86				3.77	2.76	3.05	3.50	2.41	2.87
1.5							4.41	3.78	3.76							3.70	2.26	2.97

Table 4
$\frac{\eta}{\mu_p}$ numerical values for FF and PL GMs using SE approach for MDOF structures.

$\frac{\eta}{\mu_p}$	2S-FF			4S-FF			6S-FF			2S-PL			4S-PL			6S-PL		
T[s]	BL	PO	POd	BL	PO	POd	BL	PO	POd	BL	PO	POd	BL	PO	POd	BL	PO	POd
0.3	2.80	3.21	3.09							2.64	2.74	2.83						
0.5	3.13	2.98	2.63	5.60	5.35	5.03				3.30	4.05	2.20	3.94	3.68	4.06			
1				6.25	4.75	5.32	6.78	4.76	4.77				4.87	3.94	3.89	5.16	4.41	4.23
1.5							6.08	5.97	5.21							5.3	4.27	4.22

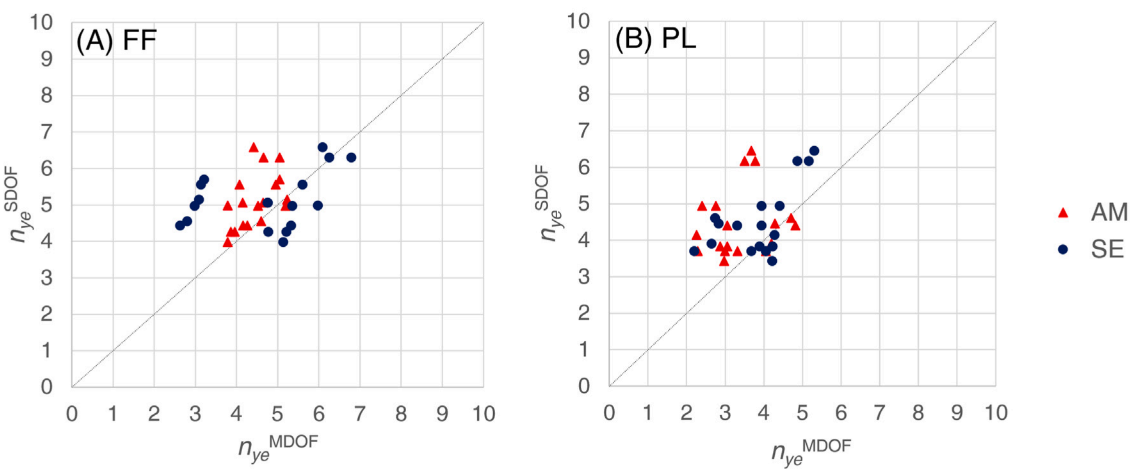

Fig. 6. n_{ye} values obtained as η/μ_p slopes, comparison of SDOF and MDOF values: (A) FF GMs set, (B) PL GMs set.

whereas the SE method similarly demonstrates a slight tendency toward underestimation but median ratios are substantially closer to unity (ranging from 0.87 to 0.97). Furthermore, the analysis of the C.o.V. reveals that both the AM and SE methods exhibit coefficients of variation consistently below 0.3.

Table 5
Median, Mean and C.o.V. of $n_{ye}^{\mathrm{MDOF}}/n_{ye}^{\mathrm{SDOF}}$.

	Median		Mean		C.o.V.	
	n_{ye}^{AM}	n_{ye}^{SE}	n_{ye}^{AM}	n_{ye}^{SE}	n_{ye}^{AM}	n_{ye}^{SE}
FF	0.91	0.97	0.88	0.92	0.12	0.28
PL	0.77	0.87	0.78	0.88	0.27	0.22

5.1.2. Descriptive Statistics of SDOF Systems

As shown in Fig. 4, the results exhibit a marked dispersion in general, which emphasizes the importance of examining the underlying variability within the analysed datasets. Fig. 7 presents the box-and-whisker plots of the n_{ye} datasets evaluated for SDOF structures subjected to FF and PL ground motions. In this graph, the target symbol denotes the median value, the box edges correspond to the 25th and 75th percentiles, and the whiskers indicate the 5th and 95th fractiles, assuming a normal distribution. Tables 6 and 7 report the logarithmic median (θ) and dispersion (β) values for the analysed samples. It is observed that the median values consistently fall within the range of 3 to 6. The BL model yields lower values, particularly at shorter periods, while the POd model systematically produces slightly lower values compared to its non-degrading counterpart. In terms of dispersion, β values range from 0.42 to 0.64, with the BL model typically showing higher variability. Furthermore, an inverse relationship is generally observed between the period and the dispersion, with longer periods associated with lower β values.

5.1.3. MDOF assessment

Figs. 8 and 9 illustrate the n_{ye} values obtained for the MDOF structures using the AM approach under the FF and PL ground motion sets, respectively. The corresponding logarithmic medians and dispersions, which complement the graphical results, are reported in Tables 8 and 9 for the FF dataset and in Tables 10 and 11 for the PL dataset. The trends observed closely align with those from the SDOF analysis: the PO and POd models yield similar median n_{ye} values, while the BL model

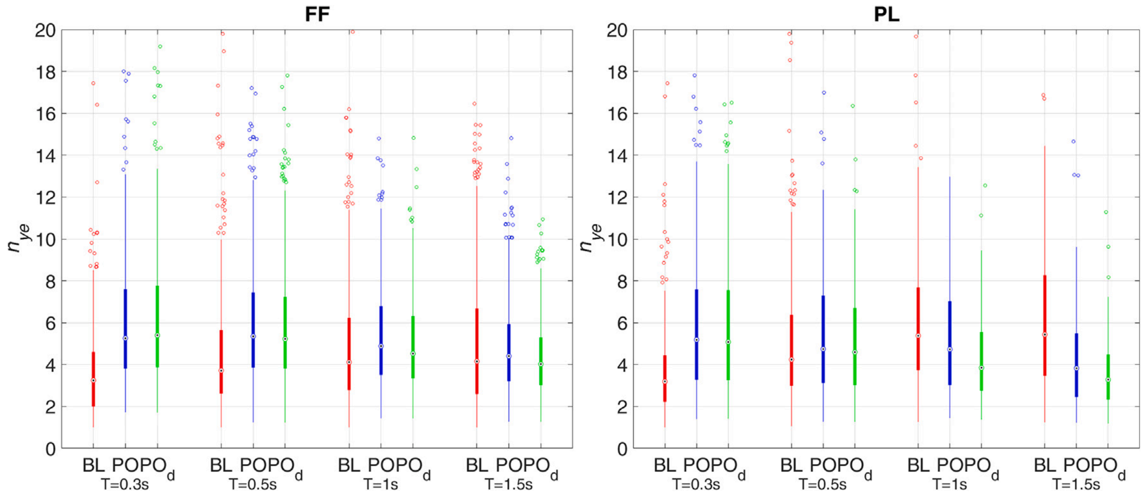

Fig. 7. n_{ye} values for SDOF structures subjected to FF and PL GMs set.

Table 6
Logarithmic median (θ) of n_{ye} values for FF and PL GMs set on SDOF structures.

θ	SDOF - FF			SDOF - PL		
T[s]	BL	PO	POd	BL	PO	POd
0.3	3.15	5.35	5.46	3.26	5.16	5.10
0.5	3.76	5.4	5.27	4.36	4.75	4.43
1	4.13	4.83	4.54	5.33	4.62	3.88
1.5	4.07	4.33	3.97	5.21	3.79	3.29

Table 7
Logarithmic standard deviation(β) of n_{ye} values for FF and PL GMs set on SDOF structures.

β	SDOF - FF			SDOF - PL		
T[s]	BL	PO	POd	BL	PO	POd
0.3	0.59	0.5	0.5	0.58	0.56	0.54
0.5	0.59	0.48	0.46	0.57	0.53	0.51
1	0.58	0.45	0.43	0.52	0.52	0.47
1.5	0.64	0.46	0.42	0.58	0.52	0.45

consistently exhibits lower values. However, for MDOF systems, the median n_{ye} values are generally smaller than those observed for the SDOF case, typically not exceeding 4. In terms of dispersion, the interquartile range remains relatively stable across the different hysteretic models, with the 75th percentile and 95th fractile consistently below 6 and 10, respectively. The logarithmic dispersions reported in Tables 9 and 11 range between 0.41 and 0.54. While these results confirm a strong correlation with equivalent SDOF systems, they also reveal that the uncertainty in the estimation of the median n_{ye} value is significant. This underscores the need for predictive equations capable of estimating n_{ye} as a function of both seismological parameters and structural properties. Moreover, it highlights the necessity of integrating this information into Energy-Based Design (EBD) methodologies through semi-probabilistic frameworks, for instance, by appropriately calibrating partial factors. To further provide a detailed comparison between the SDOF and MDOF results and assess the performance of the different MDOF evaluation approaches, Fig. 10 presents a scatter plot of the median n_{ye} values for the FF and PL GM sets. Consistently with the results in Section 5.1, the figure reveals a systematic underestimation of n_{ye} for MDOF systems when using both the AM and SE approaches. These tendencies are quantified in Table 12, which shows that the AM and SE approaches yield median ratios below 70% and 60%, respectively, with a dispersion under 40%.

Figs. 11 and 12 illustrate the distribution of yielding excursions across the storeys for the FF and PL ground motion sets, respectively. From these plots, it is evident that the distribution of yielding excursions is fairly uniform, especially in the 4-storey and 6-storey structures. It should be noted that the relatively uniform distribution of plasticity across storeys is closely related to the adopted linear force distribution. In this regard, it is not surprising that the 2-storey case yielded less satisfactory results, as a uniform (rather than linear) distribution might better represent the response of such low-rise structures. Consequently, while the current findings provide valuable insights for regular frames, further analyses incorporating alternative strength distributions, such as the 'optimal' distribution proposed by Akiyama [38], Akiyama [39] and Donaire-Ávila et al. [50] are desirable to generalize these conclusions. Research is currently underway to address this point. As previously observed, the BL model results in lower $n_{ye,i}$ values (typically between 2 and 3), while the PO and POd models show slightly higher values (between 3 and 4), with more pronounced differences under the FF ground motions. These findings demonstrate a relatively uniform ductility demand across the storeys, thus supporting the effectiveness of adopting an Arithmetic Mean (AM) for the global evaluation of the equivalent number of yielding excursions for MDOF systems. However, it is essential to distinguish between global demand characterization and local safety assessment. While the AM provides a robust statistical measure of the overall hysteretic performance (e.g., to be used in the strength reduction framework exposed in Section 5.1.5), it may inherently mask localized phenomena, such as weak-storey mechanisms, where a single storey concentrates the majority of the seismic demand. Therefore, while the AM is proposed as a representative parameter for the structural typologies investigated, its application should be complemented by localized $n_{ye,i}$ checks, particularly in cases involving significant structural irregularities or extreme pulse-like ground motions that could trigger localized failure modes.

5.1.4. Discussion

Although the results provided hereafter demonstrate a large variability within the dataset, which precludes the establishment of a definitive assessment, an attempt to provide a summary of the main trends observed is presented in the following.

- **Comparison between AM and SE methods:** The collected data indicate that, while the two methods produce comparable results

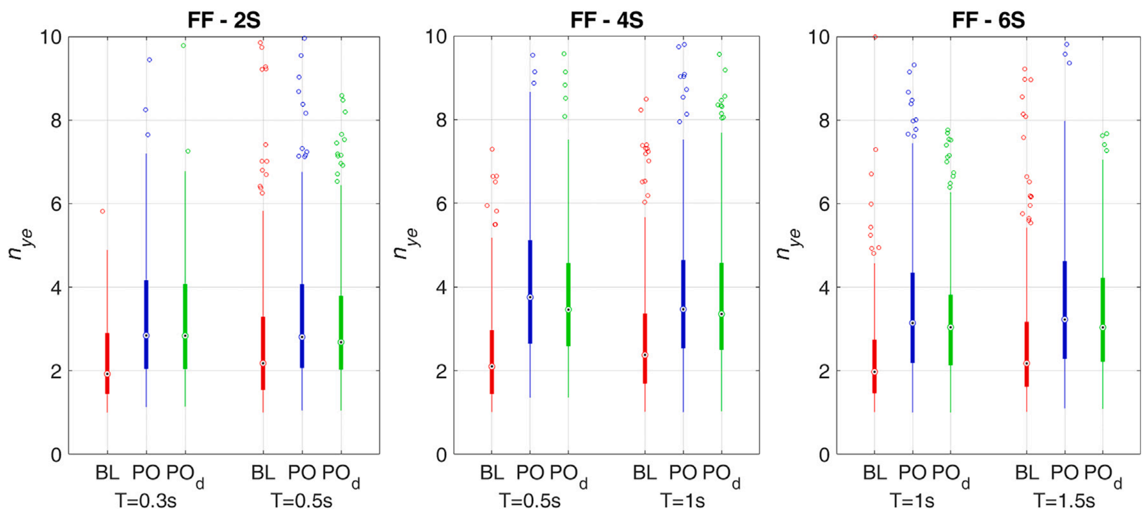

Fig. 8. n_{ye} values for MDOF structures subjected to FF GMs using the AM approach.

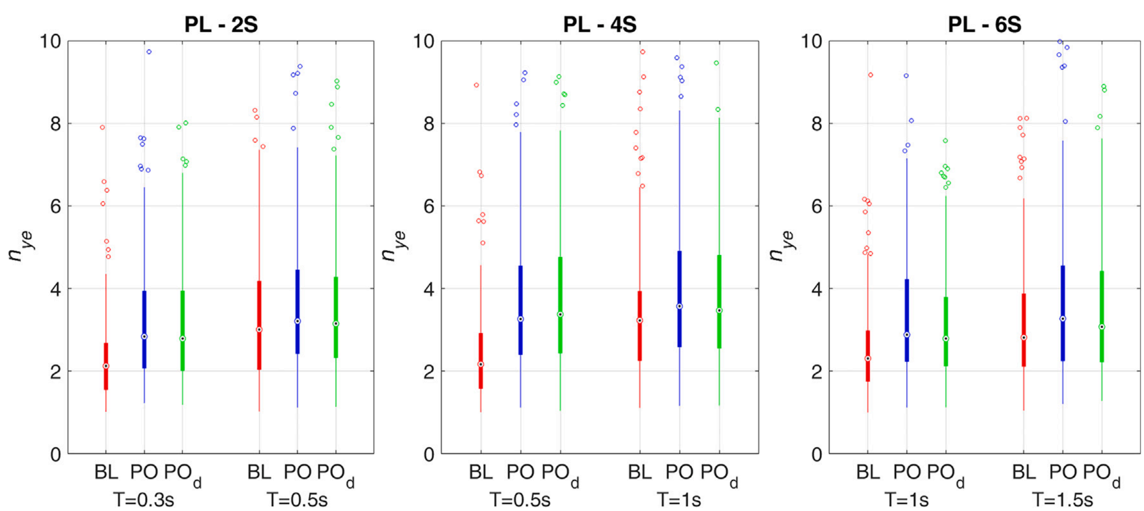

Fig. 9. n_{ye} values for MDOF structures subjected to PL GMs using the AM approach.

Table 8
Logarithmic median(θ) of n_{ye} values for FF set on MDOF structures with linear force distribution.

θ	2S			4S			6S		
T[s]	BL	PO	POd	BL	PO	POd	BL	PO	POd
0.3	2.08	2.91	2.92						
0.5	2.33	2.89	2.78	2.23	3.78	3.54			
1				2.44	3.43	3.38	2.06	3.15	2.93
1.5							2.34	3.24	3.06

Table 9
Logarithmic standard deviation (β) of n_{ye} values for FF set on MDOF structures with linear force distribution.

β	2S			4S			6S		
T[s]	BL	PO	POd	BL	PO	POd	BL	PO	POd
0.3	0.46	0.49	0.48						
0.5	0.54	0.48	0.46	0.51	0.51	0.45			
1				0.47	0.48	0.44	0.45	0.51	0.43
1.5							0.50	0.48	0.44

on average, their estimates may differ significantly on a case by case basis. Using the SDOF results as a reference, the AM method exhibits a closer agreement when comparing sample medians, whereas the SE method aligns slightly better with the η/μ based estimates, although the differences remain small. Overall, both methods appear suitable for estimating the global n_{ye} for the cases investigated, where a relatively well-distributed ductility demand is expected. However, a slight preference may be given to the AM method, owing to its simplicity and straightforward interpretation.

- **Comparison between SDOF and MDOF systems:** In general, n_{ye} values obtained for MDOF systems are lower than those obtained for SDOF systems. Nonetheless, when using the η/μ approach, the median underestimation is at most 23%, whereas the comparison based on sample medians showed underestimations of up to 46%.
- **Comparison between hysteretic models:** The values of n_{ye} obtained for the FF set using the η/μ and AM approaches range between 4.07 and 5.05 for the BL model, between 3.78 and 5.19 for the PO model, and between 3.76 and 5.23 for the POd model. The three hysteretic models therefore provide generally

Table 10
Logarithmic median (θ) of n_{ye} values for PL set on MDOF structures with linear force distribution.

θ	2S			4S			6S		
T[s]	BL	PO	POd	BL	PO	POd	BL	PO	POd
0.3	2.16	2.97	2.86						
0.5	2.93	3.25	3.15	2.20	3.45	3.43			
1				3.11	3.57	3.49	2.31	3.04	2.86
1.5							2.87	3.33	3.19

Table 11
Logarithmic standard deviation (β) of n_{ye} values for PL set on MDOF structures with linear force distribution.

β	2S			4S			6S		
T[s]	BL	PO	POd	BL	PO	POd	BL	PO	POd
0.3	0.45	0.49	0.47						
0.5	0.49	0.46	0.45	0.45	0.54	0.50			
1				0.42	0.45	0.44	0.42	0.46	0.43
1.5							0.41	0.48	0.43

comparable estimates. The only consistent trend is that the POd model yields systematically lower values than the PO model, confirming that, given the same hysteretic properties, the inclusion of degradation tends to reduce the equivalent number of yielding excursions. This result is consistent with what observed by other authors [3] and can be attributed to the inherent differences in energy dissipation mechanisms between the two models. In the degrading model (POd), the thinner hysteretic loops and the reduction in strength/stiffness lead to a substantial decrease in the total hysteretic energy E_H (and then η) compared to the non-degrading model (PO). Conversely, the maximum ductility demand is primarily influenced by the peak response and does not necessarily increase proportionally with degradation, especially when the maximum excursion occurs in the early stages of the ground motion. As a result, the ratio $n_{ye} = \eta/\mu$ tends to be lower for the POd model. A similar comparison for the PL set shows that n_{ye} varies between 3.05 and 4.81 for the BL model, 2.29 and 4.70 for the PO model, and 2.87 and 4.29 for the POd model, leading to conclusions fully consistent with those drawn for the FF case. However, when analysing the statistical samples, it becomes evident that the BL model produces markedly lower median values compared with

Table 12
Median, Mean and C.o.V. of SDOF to MDOF median n_{ye} ratio for FF and PL GMs sets.

	Median		Mean		C.o.V.	
	n_{ye}^{AM}	n_{ye}^{SE}	n_{ye}^{AM}	n_{ye}^{SE}	n_{ye}^{AM}	n_{ye}^{SE}
FF	0.63	0.54	0.67	0.57	0.25	0.20
PL	0.69	0.56	0.73	0.61	0.35	0.38

the PO and POd models. Moreover, the medians obtained with the BL model are significantly lower than the values derived from the η/μ approach, whereas the medians of the PO and POd models are broadly consistent with the η/μ estimates.

- **Comparison across structural periods:** The n_{ye} values obtained for MDOF structures using the η/μ approach and AM across the different structural periods are fairly similar in the case of FF structures, whereas they tend to decrease with increasing period for PL structures. This behaviour is consistent with the fact that the pulse-like component primarily affects more deformable, long-period systems. Indeed, as highlighted by Chen et al. [56], multipulse ground motions exhibit velocity peaks concentrated in the long-period range, which can significantly amplify structural damage metrics specifically for flexible frame structures. This concentration of impulsive energy demand promotes a structural response characterized by large peak displacements with limited cyclic reversals, directly resulting in the lower nye values observed in this study. This result appears clearly when comparing the η/μ values, but is not as evident when comparing the median values, in particular for MDOF systems.
- **Comparison between global and local n_{ye} values**: Although this comparison has been carried out only in terms of the statistical sample, the local $n_{ye,i}$ values exhibit trends that closely mirror those of the global n_{ye}. Moreover, their distribution is fairly uniform across the storeys, indicating that the global estimate effectively captures the underlying pattern of seismic energy demand at the local scale.

5.1.5. Strength reduction factor assessment

One of the primary goals of this study is to evaluate whether an improved global n_{ye} assessment can contribute to the definition of strength reduction factors adopted in structural design. To achieve this, a critical comparison is conducted between the strength reduction factors assessed using the improved method and those obtained through traditional approaches. One of the most adopted and established expression for the

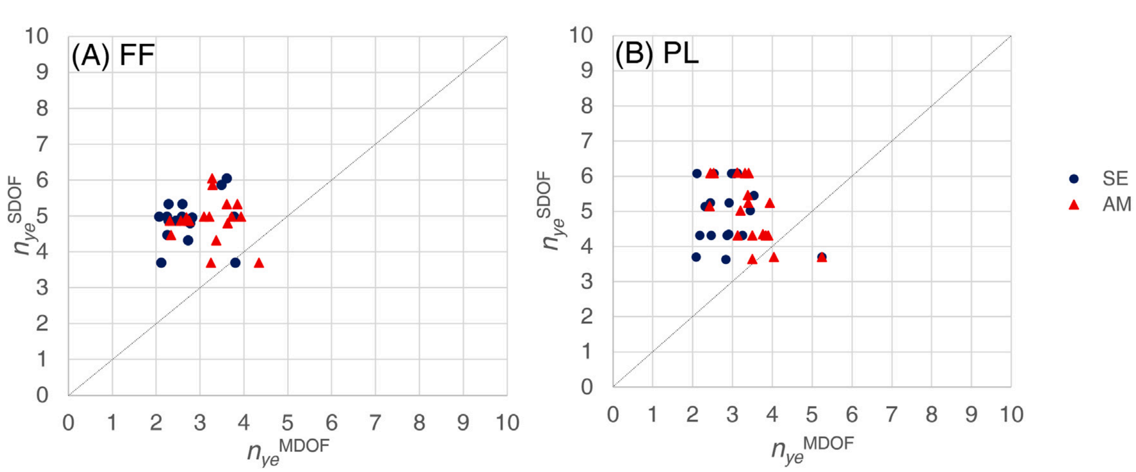

Fig. 10. Ratio of n_{ye} median values for SDOF and MDOF structures: (A) FF GMs set, (B) PL GMs set.

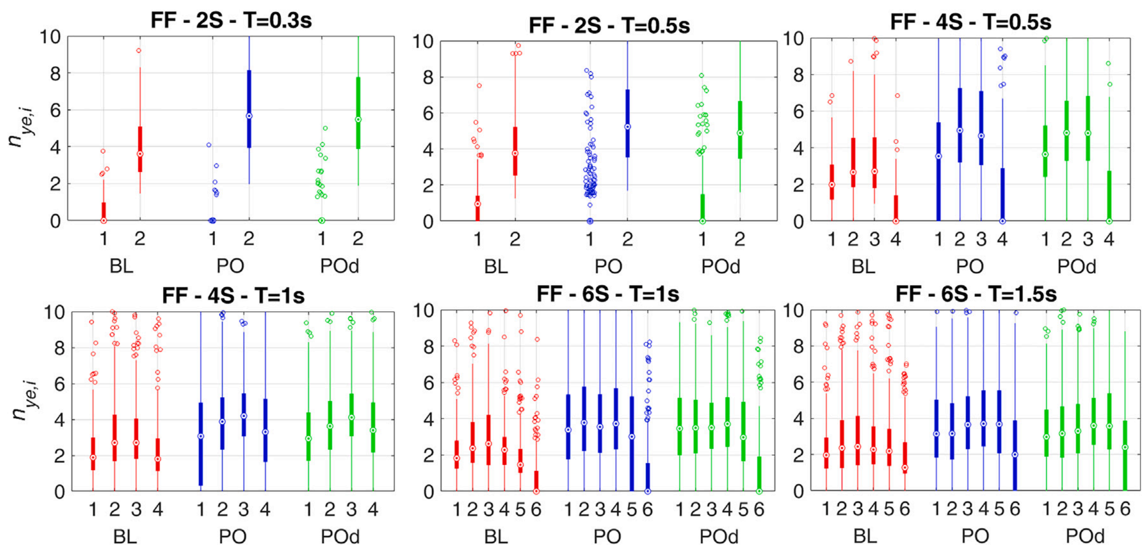

Fig. 11. $n_{ye,i}$ values for MDOF structures subjected to FF GM set.

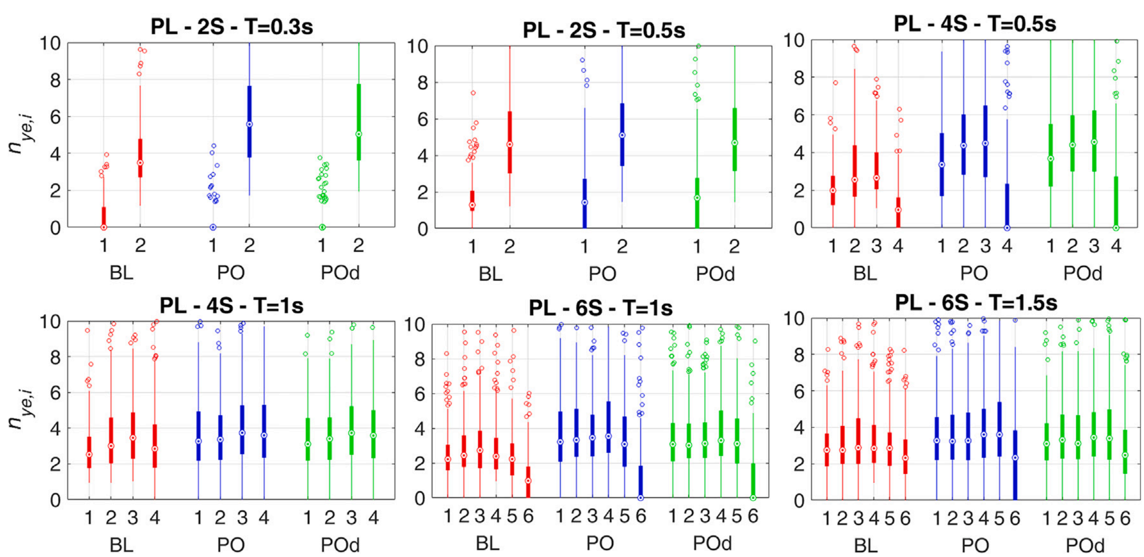

Fig. 12. $n_{ye,i}$ values for MDOF structures subjected to PL GM set.

strength reduction factor has been proposed by Veletsos and Newmark [57]:

$$\frac{A_p}{A_e} = \frac{1}{\sqrt{2\mu_p + 1}} \tag{15}$$

where A_p and A_e are the maximum force in a elasto-plastic and perfectly elastic system, respectively. As an alternative to Eq. (15), Veletsos and Newmark [57] proposed also the well-known Equal Displacement Approximation (EDA), which can be expressed as follows:

$$\frac{A_p}{A_e} = \frac{1}{\mu} \tag{16}$$

As already pointed out by Benavent-Climent et al. [11] these relationships are derived from an energy balance that does not explicitly account for the number of motion reversal and, thus, the n_{ye}. By introducing the number of equivalent cycles into the calculations, a modified expression for A_p/A_e can be provided:

$$\frac{A_p}{A_e} = \frac{1}{\sqrt{(2n_{ye}\mu_p + 1)}} \tag{17}$$

Benavent-Climent et al. [11] also demonstrated that the use of Eq. (17) leads to an overestimation of the ductility demand for a given strength reduction factor or, equivalently, the same target ductility level can be achieved by adopting higher strength reduction factors. It is worth noting that Eq. (15) becomes mathematically equivalent to Eq. (17) when $n_{ye} = 1$; however, for larger n_{ye} values, Eq. (15) results in a strong underestimation of the strength reduction factors. In such cases, Benavent-Climent et al. [11] further showed that Eq. (16) yields smaller discrepancies when compared to Eq. (17).

This problem is investigated herein by comparing the A_p/A_e values obtained from time-history analyses of the case study structures (i.e., "A_p/A_e TH") with those calculated using Eqs. (16) and (17) (i.e., "A_p/A_e Design"), based on the EDA and the Considering Energy Equivalence

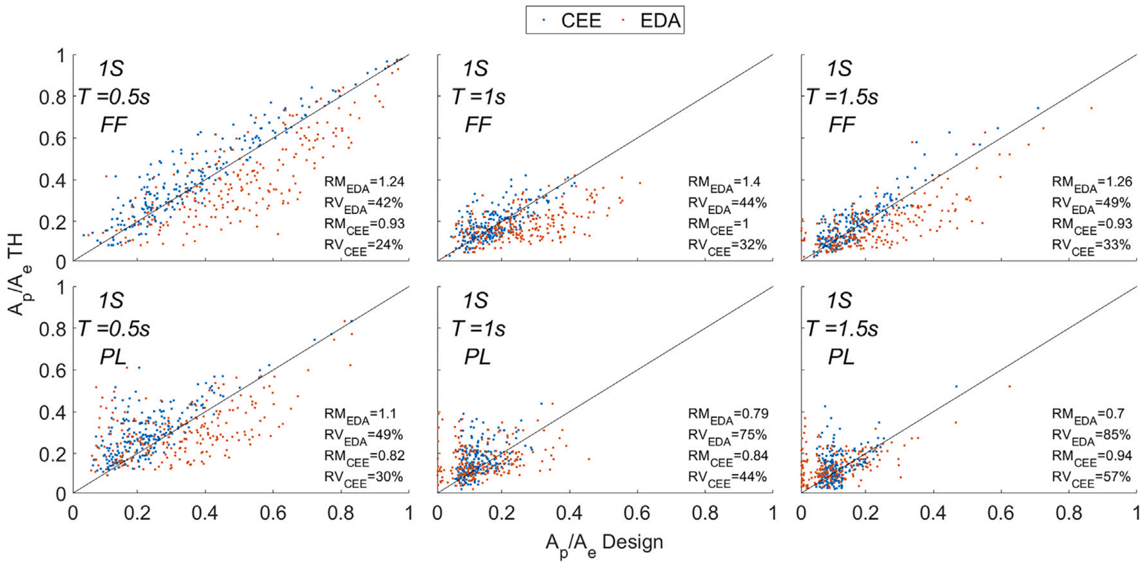

Fig. 13. Ratio between the maximum base shear of the systems assessed through plastic analyses (A_p) and linear analyses with a strength reduction factor (A_e): SDOF structures case studies with the BL model.

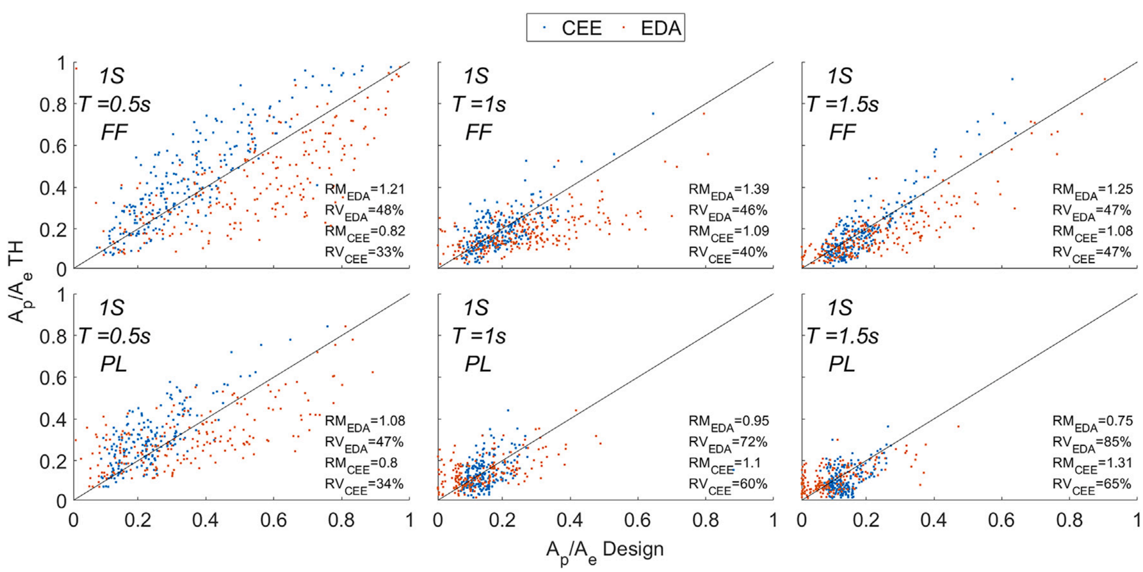

Fig. 14. Ratio between the maximum base shear of the systems assessed through plastic analyses (A_p) and linear analyses with a strength reduction factor (A_e): SDOF structures case studies with the PO model.

(CEE) approaches, respectively. For this comparative assessment, the ductility values recorded during the NLTHAs, along with the n_{ye} values presented in the previous section, are used as input parameters for both Eqs. (16) and (17). For MDOF structures, the average ductility across floors (i.e., $\overline{\mu}$) and the n_{ye} values determined using the AM approach are considered.

Figs. 13–15 show scatterplots comparing the values of A_p/A_e obtained from time-history analyses ("A_p/A_e TH") against those calculated using the design equations ("A_p/A_e Design") for SDOF structures modelled with the BL, PO, and POd approaches, respectively. To evaluate the accuracy of the EDA and CEE methods, each figure also reports the median value (RM) and coefficient of variation (RV) of the ratio between A_p/A_e TH and A_p/A_e Design. For the BL model (Fig. 13), the RM values obtained with the CEE method are close to unity under the FF GM set while those using the EDA method exceed 1.2. Also, the RV values are significantly lower when using CEE. In the case of the PL GM set, the RV remains consistently smaller with CEE, and RM values are generally nearer to 1, except for the 2-storey structure with a period $T = 0.5\,s$. For the PO and POd models, Figs. 14 and 15 show that the CEE approach consistently leads to smaller RV values compared to EDA across all analyzed datasets and periods, however, for the RM parameter, the superiority of the CEE approach is systematically observed for the FF dataset, whereas for PL records, the results are more varied.

Figs. 16–18 present the scatterplots comparing A_p/A_e, obtained from NLTHAs (A_p/A_e TH), with design calculations (A_p/A_e Design) for MDOF structures modelled with the BL, PO, and POd approaches, respectively. The results demonstrate that the CEE approach consistently reduces RV compared to the EDA approach across all investigated cases. For the 4S and 6S structures, RM also remains remarkably close to unity,

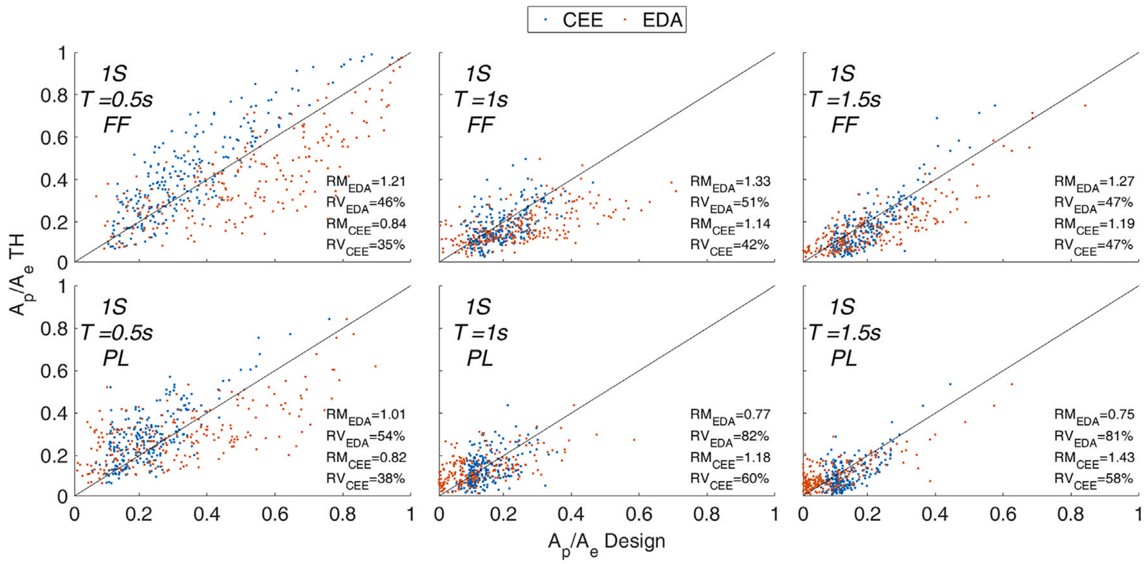

Fig. 15. Ratio between the maximum base shear of the systems assessed through plastic analyses (A_p) and linear analyses with a strength reduction factor (A_e): SDOF structures case studies with POd model.

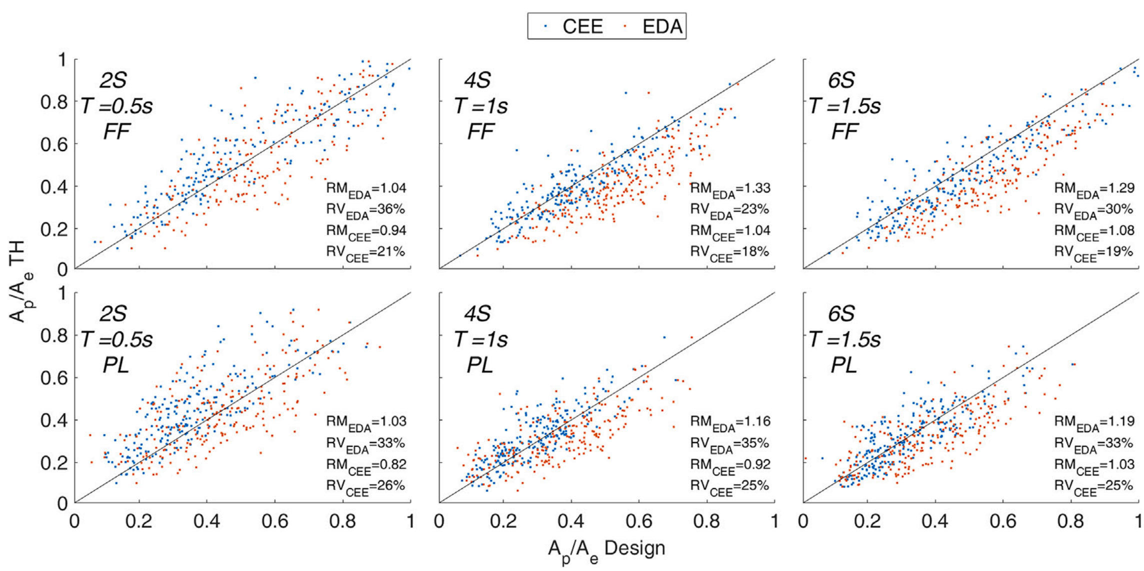

Fig. 16. Ratio between the maximum base shear of the systems assessed through plastic analyses (A_p) and linear analyses with a strength reduction factor (A_e): MDOF structures case studies with the BL model.

highlighting a significant improvement in the prediction of strength reduction factors. This confirms that the global n_{ye} AM method is highly effective when there is a strong correlation between global and local energy demands. However, this improvement in RM is not observed for the 2S cases, where the CEE approach does not provide a better mean estimation compared to the EDA. As previously discussed, this lack of improvement is likely due to the lateral force distribution being less suitable for this specific typology, which leads to a poorer agreement between global and local demands. Despite this, the overall consistency of Eq. (17) across the majority of cases confirms the validity of the proposed global n_{ye} AM values for representing the structural energy demand in MDOF systems.

Ultimately, incorporating energy-based metrics into international standards, even within traditional force-based frameworks, can enhance the predictive reliability of seismic assessments. This transition not only ensures a more consistent level of structural safety but also promotes cost-effective design by reducing the overconservatism associated with traditional approaches.

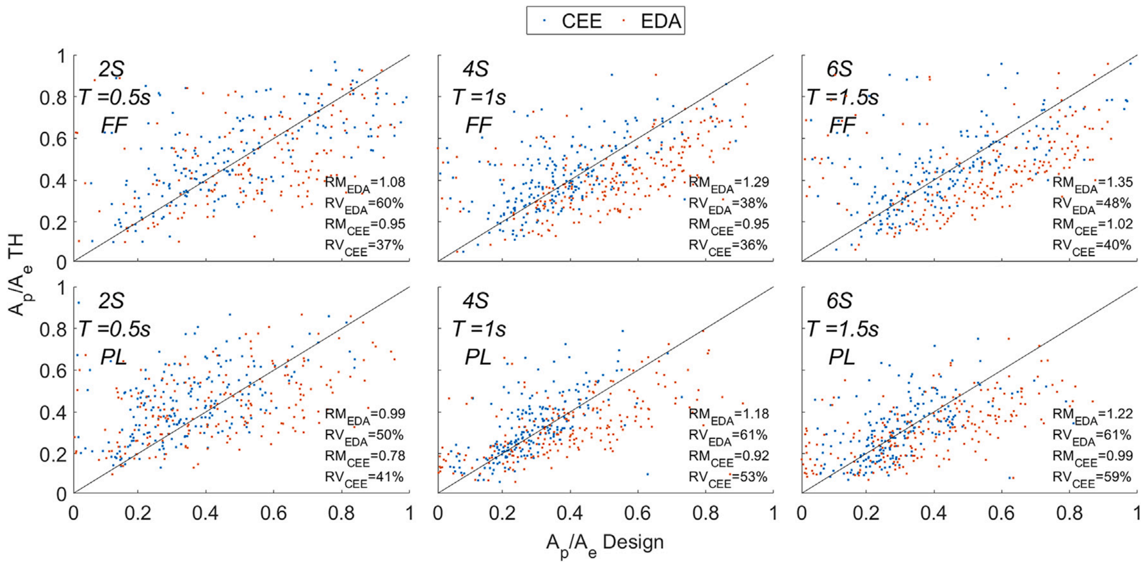

Fig. 17. Ratio between the maximum base shear of the systems assessed through plastic analyses (A_p) and linear analyses with a strength reduction factor (A_e): MDOF structures case studies with the PO model.

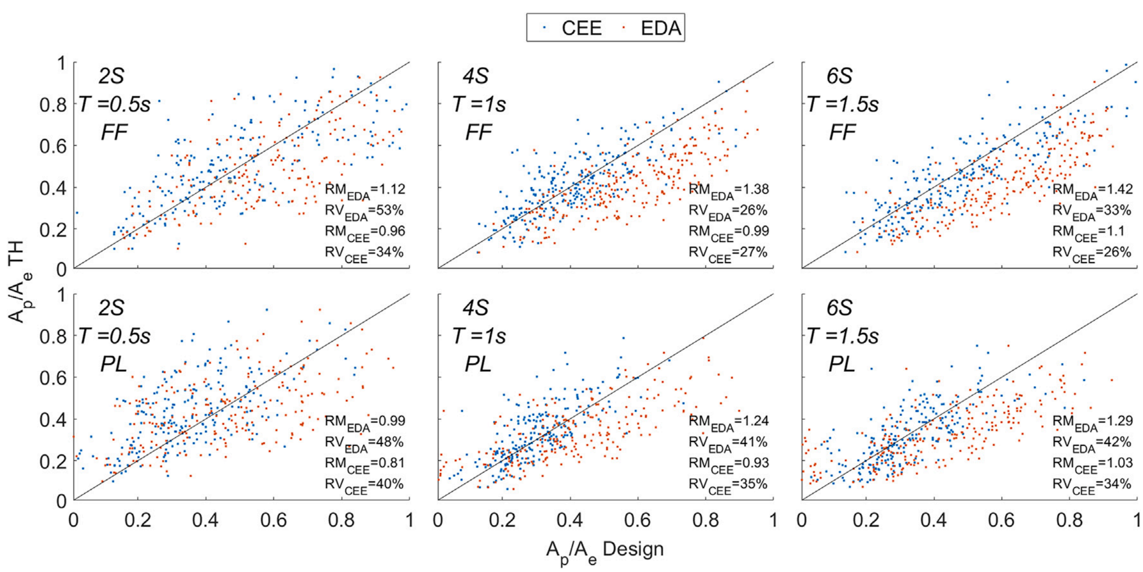

Fig. 18. Ratio between the maximum base shear of the systems assessed through plastic analyses (A_p) and linear analyses with a strength reduction factor (A_e): MDOF structures case studies with POd model.

6. Conclusion

This work presents a comprehensive framework for the assessment of the equivalent number of yielding excursions (n_{ye}) in multi-storey structures, as a fundamental parameter to quantify the cumulative damage sustained by a structure in terms of plastic deformation cycles. The study systematically investigates the influence of different hysteretic models, including the Ibarra-Medina-Krawinkler Bilinear (BL), Peak-Oriented (PO), and Peak-Oriented with degradation (POd) models, and two ground motion datasets, encompassing Far-Field (FF) and Near-Field Pulse-Like (PL) records. Nonlinear time-history analyses are performed on 2, 4, and 6-storey structures with fundamental periods ranging from 0.3 s to 1.5 s, benchmarked against equivalent SDOF systems. To extend the n_{ye} concept to MDOF systems for applications within Energy-Based Design (EBD) frameworks, this study evaluates both storey-specific values ($n_{ye,i}$) and a global, system-level n_{ye} parameter. This latter is derived using two distinct methods: the Arithmetic Mean (AM), which averages local energy demands across all storeys, and the SDOF Equivalence (SE), which defines n_{ye} through an equivalent SDOF system at the fundamental period of vibration.

The main findings of this study can be summarized as follows:

- Both AM and SE methods yield consistent estimates of global energy demand, particularly for the regular 4- and 6-storey structures analyzed. Within the scope of these configurations, the AM approach is preferred for practical applications due to its simplicity.
- n_{ye} values for MDOF systems are systematically lower than those observed in equivalent SDOF models, with sample medians showing reductions of up to 46% though smaller differences were found when analyzing slopes in the η/μ_p plane (up to 23%).
- When evaluated as the slope in the η/μ_p plane, n_{ye} for MDOF systems using the AM approach ranges between 3.5 and 5.5 for FF records and 2.0–5.0 for PL sets. While median values reside between 2 and 4, the observed log-normal dispersions remain

substantial (between 0.4 and 0.6). These results show strong alignment with the findings of [37,38], thus confirming the reliability of the proposed framework across a broader range of ground motions and structural configurations. Moreover, the storey-wise $n_{ye,i}$ medians (ranging from 3 to 4) align closely with the reference value of 4 proposed in the upcoming Eurocode 8.

- The three investigated hysteretic models (BL, PO, and POd) yield comparable results, with two distinct trends emerging. First, a systematic decrease in n_{ye} is observed for the POd model relative to the PO model due to the effects of cyclic degradation. Second, the median values of both global n_{ye} and local $n_{ye,i}$ for the BL model are consistently lower than those of the PO and POd models. Interestingly, differences between models vanish when n_{ye} is estimated as the slope in the η/μ_p plane.
- The proposed global n_{ye} values significantly enhance the predictive capability of strength reduction factors compared to the traditional Equal Displacement Approximation (EDA). This improvement is particularly evident for the 4- and 6-storey structures, where the regular seismic response ensures a strong correlation between global and local energy demands.

In summary, the results confirm that for regular MDOF structures, the global n_{ye} evaluated through the AM technique provides a robust and effective characterization of the overall cyclic demand, serving as a robust synthetic parameter for EBD frameworks. On the other hand, the significant dispersions observed highlight the need for predictive models of n_{ye} that incorporate the specific seismological and structural features. Moreover, the significant dispersion observed also underscores the necessity of a probabilistic framework to define appropriate partial factors to be used, for example, within semi-probabilistic design approaches. To this end, further investigations into these aspects constitute a key component of ongoing research.

CRediT authorship contribution statement

Raffaele Laguardia: Writing – review & editing, Writing – original draft, Visualization, Validation, Methodology, Investigation, Formal analysis, Data curation, Conceptualization. **Giulia Angelucci:** Writing – review & editing, Writing – original draft, Visualization, Validation, Methodology, Investigation, Data curation, Conceptualization. **Fabrizio Mollaioli:** Writing – review & editing, Visualization, Validation, Supervision, Resources, Project administration, Methodology, Investigation, Conceptualization.

Declaration of competing interest

The authors declare that they have no known competing financial interests or personal relationships that could have appeared to influence the work reported in this paper.

References

[1] Housner GW. Limit design of structures. 1956.
[2] Akiyama H, Kato B. Energy concentration of multistory buildings. In: Proceedings of 7th WCEE, Istanbul, vol. 4; 1980. p. 553–60.
[3] Akiyama H. Earthquake-resistant limit-state design for buildings. University of Tokyo Press; 1985.
[4] Akiyama H. Earthquake resistant design based on energy concept. In: Proceedings of ninth world conference on earthquake engineering, Tokyo-Kyoto (Japan), vol. 5; 1988. p. 905–10.
[5] Berg GV, Thomaides SS. Energy consumption by structures in strong-motion earthquakes. In: Proceedings of the second world conference on earthquake engineering, vol. 2; 1960. p. 681–97.
[6] Tembulkar JM, Nau JM. Inelastic modeling of seismic energy dissipation. J Struct Eng 1987;113:1373–7.
[7] Jennings PC. Earthquake response of a yielding structures. J Eng Mech Div 1965;91:41–68.
[8] Uang C, Bertero VV. Evaluation of seismic energy in structures. Earthq Eng Struct Dyn 1990;19:77–90.
[9] De Angelis M, Angelucci G, Quaranta G, Mollaioli F, Tesfamariam S. Energy-based framework for designing pinned rocking systems with dissipative devices. J Build Eng 2025;112:113495.
[10] Tropea GA, Angelucci G, Bernardini D, Quaranta G, Mollaioli F. New energy-based methodology to characterize nonlinear seismic response. Eng Struct 2025;325:119488.
[11] Benavent-Climent A, Donaire-Ávila J, Mollaioli F. Key points and pending issues in the energy-based seismic design approach. In: Energy-based seismic engineering. Springer International Publishing; 2021. p. 151–68.
[12] Mollaioli F, Benavent-Climent A, Takewaki I. Editorial: energy-based seismic engineering. Front Built Environ 2023;9.
[13] Gholami N, Garivani S, Askariani SS. State-of-the-art review of energy-based seismic design methods. Arch Comput Methods Eng 2022;29:1965–96.
[14] Somerville P, Graves R. Conditions that give rise to unusually large long period ground motions. Struct Des Tall Build 1993;2:211–32.
[15] Archuleta RJ, Hartzell SH. Effects of fault finiteness on near-source ground motion. Bull Seismol Soc Am 1981;71:939–57.
[16] Fujii K. Bidirectional seismic energy input to an isotropic nonlinear one-mass two-degree-of-freedom system. Buildings 2021;11:143.
[17] Kalkan E, Kunnath SK. Effective cyclic energy as a measure of seismic demand. J Earthquake Eng 2007;11:725–51.
[18] Hori N, Inoue N. Damaging properties of ground motions and prediction of maximum response of structures based on momentary energy response. Earthq Eng Struct Dyn 2002;31:1657–79.
[19] Bray JD, Rodriguez-Marek A. Characterization of forward-directivity ground motions in the near-fault region. Soil Dyn Earthq Eng 2004;24:815–28.
[20] Mollaioli F, Bruno S, Decanini LD, Panza GF. Characterization of the dynamic response of structures to damaging pulse-type near-fault ground motions. Meccanica 2006;41:23–46.
[21] Mavroeidis GP. A mathematical representation of near-fault ground motions. Bull Seismol Soc Am 2003;93:1099–131.
[22] Baker JW. Quantitative classification of near-fault ground motions using wavelet analysis. Bull Seismol Soc Am 2007;97:1486–501.
[23] Lu Y, Panagiotou M. Characterization and representation of pulse-like ground motions using cumulative pulse extraction via wavelet analysis. Berkeley: Technical Report UCB/SEMM-2013/01; 2013.
[24] Quaranta G, Mollaioli F. Analysis of near-fault pulse-like seismic signals through variational mode decomposition technique. Eng Struct 2019;193:121–35.
[25] Mazza F. Nonlinear incremental analysis of fire-damaged r.c. Base-isolated structures subjected to near-fault ground motions. Soil Dyn Earthq Eng 2015;77:192–202.
[26] Alonso-Rodríguez A, Miranda E. Assessment of building behavior under near-fault pulse-like ground motions through simplified models. Soil Dyn Earthq Eng 2015;79:47–58.
[27] Quaranta G, Angelucci G, Mollaioli F. Near-fault earthquakes with pulse-like horizontal and vertical seismic ground motion components: analysis and effects on elastomeric bearings. Soil Dyn Earthq Eng 2022;160:107361.
[28] Angelucci G, Quaranta G, Mollaioli F, Kunnath SK. Interpretable machine learning models for displacement demand prediction in reinforced concrete buildings under pulse-like earthquakes. J Build Eng 2024;95:110124.
[29] McCabe SL, Hall WJ. Evaluation of structural response and damage resulting from earthquake ground motion. Technical Report 1987.
[30] Kunnath SK, Chai YH. Cumulative damage-based inelastic cyclic demand spectrum. Earthq Eng Struct Dyn 2004;33:499–520.
[31] Dutta A, Mander JB. Energy based methodology for ductile design of concrete columns. J Struct Eng 2001;127(12):1374–81.
[32] Malhotra PK. Cyclic-demand spectrum. Earthq Eng Struct Dyn 2002;31:1441–57.
[33] Manson SS. Behavior of materials under conditions of thermal stress. NACA - Technical Note 2933 1954.
[34] Morillas L, Escolano-Margarit D. Estimation of cyclic demand in metallic yielding dampers installed on frame structures. Appl Sci (Basel) 2020;10(12):4364.
[35] Zhang K, Zuo Z, Gong M, Wang X, Zhao Y, Liu B. The influence of forward-directivity pulse-like ground motion orientation angles on structural collapse capacity. Soil Dyn Earthq Eng 2025;191:109280.
[36] Zuo Z, Gong M, Sun J, Zhang H. Seismic performance of RC frames with different column-to-beam flexural strength ratios under the excitation of pulse-like and non-pulse-like ground motion. Bull Earthquake Eng 2021;19:5139–59.
[37] Climent AB, Donaire-Ávila J, Mollaioli F. Comparison of energy-based, force-based and displacement-based seismic design approaches for RC frames in the context of 2G of Eurocode 8. In: Lecture notes in civil engineering. Springer Nature Switzerland, Cham; 2023. p. 98–111.
[38] Akiyama H. Earthquake-resistant design method for buildings based on energy balance. Tokyo (in Japanese): Gihodo Shuppan; 1999.
[39] Akiyama H. Collapse modes of structures under strong motions of earthquake. Annals of Geophysics; 2002.
[40] Manfredi G. Evaluation of seismic energy demand. Earthq Eng Struct Dyn 2001;30:485–99.
[41] Manfredi G, Polese M, Cosenza E. Cumulative demand of the earthquake ground motions in the near source. Earthq Eng Struct Dyn 2003;32:1853–65.
[42] Benavent-Climent A, Oliver-Saiz E, Donaire-Ávila J. Seismic retrofitting of RC frames combining metallic dampers and limited strengthening with FRP/SRP applying energy-based methods. Soil Dyn Earthq Eng 2024;177:108432.
[43] Donaire-Ávila J, Benavent-Climent A, Lucchini A, Mollaioli F. Energy based seismic design methodology: a preliminary approach. In: Proceeding of 16th WCEE; 2017.
[44] Benavent-Climent A. From conventional to innovative approaches in seismic engineering: buildings with energy dissipation systems and the upcoming second generation of eurocode-8. In: Springer proceedings in earth and environmental sciences. Cham: Springer International Publishing; 2022. p. 379–97.
[45] De Sortis A, Bazzurro P, Mollaioli F, Bruno S. Influenza delle tamponature sul rischio sismico degli edifici in calcestruzzo armato. In: Proceedings of the Italian conference on seismic engineering ANIDIS 2007. Pisa (IT) (in Italian); 2007.

[46] Mazzoni S, McKenna F, Scott MH, Fenves GL. OpenSees command language manual, Pacific earthquake engineering research (PEER). Center; 2007.
[47] Angelucci G, Mollaioli F, Quaranta G. Correlation between energy and displacement demands for infilled reinforced concrete frames. Front Built Environ 2023;9.
[48] Lignos Dimitrios G, Helmut K. Deterioration modeling of steel components in support of collapse prediction of steel moment frames under earthquake loading. J Struct Eng 2011;137:1291–302.
[49] Lignos Dimitrios G, Helmut K. Development and utilization of structural component databases for performance-based earthquake engineering. J Struct Eng 2013;139:1382–94.
[50] Donaire-Ávila J, Lucchini A, Benavent-Climent A, Mollaioli F. New optimum distribution of lateral strength of shear-type buildings for uniform damage. Struct Eng Mech 2020;76:279–91.
[51] Jalayer F, Ebrahimian H, Miano A, Manfredi G, Sezen H. Analytical fragility assessment using unscaled ground motion records. Earthq Eng Struct Dyn 2017;46:2639–63.
[52] Chen G, Yang J, Liu Y, Kitahara T, Beer M. An energy-frequency parameter for earthquake ground motion intensity measure. Earthq Eng Struct Dyn 2023;52:271–84.
[53] Gao Q, Quaranta G, Mollaioli F, Chang Z, Monti G. A novel framework for parameterization and simulation of near-fault velocity-pulses. Mech Syst Signal Process 2026;245:113847.
[54] AlShawa O, Angelucci G, Mollaioli F, Quaranta G. Quantification of energy-related parameters for near-fault pulse-like seismic ground motions. Appl Sci (Basel) 2020;10:7578.
[55] Aljawhari K, Gentile R, Freddi F, Galasso C. Effects of ground-motion sequences on fragility and vulnerability of case-study reinforced concrete frames. Bull Earthquake Eng 2021;19:6329–59.
[56] Chen G, Yang J, Wang R, Li K, Liu Y, Beer M. Seismic damage analysis due to near-fault multipulse ground motion. Earthq Eng Struct Dyn 2023;52:5099–116.
[57] Veletsos A, Newmark NM. Effect of inelastic behavior on the response of simple systems to earthquake motions. 1960.